

Weierstraß-Institut
für Angewandte Analysis und Stochastik
Leibniz-Institut im Forschungsverbund Berlin e. V.

Preprint

ISSN 2198-5855

Scattering of general incident beams by diffraction gratings

Gunther Schmidt

submitted: December 21, 2016

Weierstrass Institute
Mohrenstr. 39
10117 Berlin
Germany
E-Mail: gunther.schmidt@wias-berlin.de

No. 2355
Berlin 2016



2010 *Mathematics Subject Classification.* 78A45, 78A40, 65D30.

Key words and phrases. Diffraction, periodic structure, beam incidence, adaptive algorithm, cubature.

Edited by
Weierstraß-Institut für Angewandte Analysis und Stochastik (WIAS)
Leibniz-Institut im Forschungsverbund Berlin e. V.
Mohrenstraße 39
10117 Berlin
Germany

Fax: +49 30 20372-303
E-Mail: preprint@wias-berlin.de
World Wide Web: <http://www.wias-berlin.de/>

Abstract

The paper is devoted to the electromagnetic scattering of arbitrary time-harmonic fields by periodic structures. The Floquet-Fourier transform converts the full space Maxwell problem to a two-parameter family of diffraction problems with quasiperiodic incidence waves, for which conventional grating methods become applicable. The inverse transform is given by integrating with respect to the parameters over an infinite strip in \mathbb{R}^2 . For the computation of the scattered fields we propose an algorithm, which extends known adaptive methods for the approximate calculation of multiple integrals. The novel adaptive approach provides autonomously the expansion of the incident field into quasiperiodic waves in order to approximate the scattered fields within a prescribed error tolerance. Some application examples are numerically examined.

1 Introduction

Periodic structures are widely used in microwave, millimeter-wave, and optical wave regions because of various effects; for example, wave reflection, wavelength or polarization selectivity, mode conversion. Therefore, electromagnetic scattering from periodic structures has been extensively studied, and many analytical and numerical approaches have been developed to analyze the scattering problems when a plane wave is incident on a periodic structure. In this case the scattered waves propagate to discrete directions, and the approaches use the fact that the electromagnetic fields are quasiperiodic. This means that each field component is a product of a periodic function and an exponential phase factor. This allows to reduce the analysis region to the single periodicity cell.

The present paper is devoted to the case that an arbitrary time-harmonic field is incident on the periodic structure. Problems of this kind are not quasiperiodic, therefore they cannot be reduced to a single periodic problem. However, if the incidence field can be well approximated by a superposition of a finite number of incoming plane waves, then superposing all the scattered fields for each plane wave component will hopefully lead to a good approximation of the total scattered fields for the original problem. Then the scattering of arbitrary incidence fields is reduced to several diffraction problems with quasiperiodic wave incidence. This approach is quite common in the optics community, and the problem is addressed in a number of papers for 2- and 3-dimensional problems, mainly for Gaussian beam illumination of gratings, for example [16], [3], [17], [18].

The accuracy and computational complexity of this approach is obviously determined by the quality of the plane wave approximations of the total scattered fields, which depend nonlinearly on the geometry and material parameters of the periodic structure. Therefore accurate approximations of the incident field by plane waves do not ensure in general that the scattered fields are well approximated. Instead, the approximation method for the scattered field should perform the expansion of the incidence field, the input, such that the output, the approximation of the scattered fields, is within a given tolerance. This task reminds of adaptive integration algorithms, which ensure that the calculated integral value is within a given tolerance, even if there is not much known about the integrand function.

The aim of this paper is to build a firm foundation for the reliable approximation of scattered fields. We concentrate on the scattering of arbitrary incident fields in \mathbb{R}^3 , which is the more realistic situation even for

structures, homogeneous in one space direction. For this purpose, we apply the Floquet-Fourier transform to Maxwell's equations and derive a two-parameter family of so-called conical diffraction problems, the scattering of quasiperiodic waves with oblique incidence by the periodic structure. The scattered fields are obtained using the inverse Floquet-Fourier transform of the results of these problems, which can be solved with conventional grating methods. But the inverse transform is given by integrating with respect to the parameters over a semi-infinite domain in \mathbb{R}^2 . Thus a cubature of this 2d-integral provides an approximation of the scattered fields, where the determination of the integrand at one cubature node requires the solution of a conical diffraction problem.

For the reliability of the computed scattered fields we propose an adaptive algorithm, which extends adaptive methods for the approximate calculation of multiple integrals. The new method determines autonomously, depending on local error estimators, the cubature nodes, for which the incident field is approximated by a quasiperiodic wave via Floquet-Fourier transform and the corresponding conical diffraction problems is solved.

In Section 2 we consider the Maxwell problem for beam scattering by gratings and discuss the transformation to the two-parameter family of conical diffraction problems. Section 3 describes the field computation and the adaptive algorithm. Some examples of beam scattering by a lamellar grating are given in Section 4.

2 Formulation

2.1 Maxwell equations

We consider a general periodic structure in \mathbb{R}^3 , which is infinitely wide, contained in a layer $\{(x_1, x_2, x_3) : |x_2| < H\}$, and invariant in one spatial direction, say x_3 . It separates two regions filled with media of constant permittivity and permeability. In the sequel the region above the inhomogeneous structure, containing a halfspace $\{x_2 > H\}$, is denoted by G_+ , the region below the structure by G_- . The structure consists of different homogeneous materials, characterized by permittivity and permeability functions ε and μ , which are piecewise constant, periodic in x_1 and do not depend on x_3 . Thus the piecewise constant functions $\varepsilon(x_1, x_2)$ and $\mu(x_1, x_2)$ characterize the geometry, inside the inhomogeneous structure they are periodic in x_1 and outside they are constant with $\varepsilon(x_1, x_2) = \varepsilon_{\pm}$ and $\mu(x_1, x_2) = \mu_{\pm}$ in G_{\pm} .

In practice, the period d of the structures under consideration is comparable with the wavelength $\lambda = 2\pi c/\omega$ of incoming electromagnetic field, where c denotes the speed of light. Throughout the paper, we deal with only time-harmonic fields, assuming a time dependence in $\exp(-i\omega t)$. For notational convenience we will change the length scale by a factor of $2\pi/d$, such that the grating becomes 2π -periodic: $\varepsilon(x_1 + 2\pi, x_2) = \varepsilon(x_1, x_2)$, $\mu(x_1 + 2\pi, x_2) = \mu(x_1, x_2)$. Note that this is equivalent to multiplying the frequency ω by $d/2\pi$, in the following we denote this modified frequency $\tilde{\omega} = \omega d/2\pi$.

The periodic structure is illuminated from above by an electromagnetic field

$$\mathbf{E}^{inc}(x_1, x_2, x_3) e^{-i\tilde{\omega}t}, \quad \mathbf{H}^{inc}(x_1, x_2, x_3) e^{-i\tilde{\omega}t}.$$

Here we assume the existence of $H_i > H$, such that $\mathbf{E}^{inc}(x_1, x_2, x_3)$ for $x_2 < H_i$ can be represented by the integral

$$\mathbf{E}^{inc}(\mathbf{x}) = -\frac{1}{2\pi} \nabla \times \int_{X_2=H_i} \frac{e^{i\kappa_+|\mathbf{x}-\mathbf{X}|}}{|\mathbf{x}-\mathbf{X}|} \mathbf{F}(X_1, X_3) dX_1 dX_3, \quad (2.1)$$

where we denote $\mathbf{x} = (x_1, x_2, x_3)$, $\mathbf{X} = (X_1, X_2, X_3)$, $\kappa_+ = \tilde{\omega} \sqrt{\varepsilon_+ \mu_+}$ and $\mathbf{F} = (F_1, 0, F_3)^T$ is a suitable vector-function. This is the well-known integral representation of the electric field in the lower half-space $\{x_2 < H_i\}$ with the tangential components $\mathbf{E}_1^{inc}(x_1, H_i, x_3) = -F_3(x_1, x_3)$ and $\mathbf{E}_3^{inc}(x_1, H_i, x_3) = F_1(x_1, x_3)$. Then the incoming magnetic field is given by

$$\mathbf{H}^{inc}(\mathbf{x}) = \frac{i}{2\pi\tilde{\omega}\mu_+} \nabla \times \nabla \times \int_{X_2=H_i} \frac{e^{i\kappa_+|\mathbf{x}-\mathbf{X}|}}{|\mathbf{x}-\mathbf{X}|} \mathbf{F}(X_1, X_3) dX_1 dX_3. \quad (2.2)$$

The field is scattered by the grating structure to a scattered field $(\mathbf{E}^s, \mathbf{H}^s) e^{-i\tilde{\omega}t}$. The aim of the paper is the efficient computation of this scattered field outside the layer $\{(x_1, x_2, x_3) : |x_2| < H\}$.

Dropping the factor $e^{-i\tilde{\omega}t}$, the total field is given by

$$\mathbf{E} = \begin{cases} \mathbf{E}^{inc} + \mathbf{E}^s, \\ \mathbf{E}^s, \end{cases}, \quad \mathbf{H} = \begin{cases} \mathbf{H}^{inc} + \mathbf{H}^s, & \text{in } G_+ \cap \{x_2 < H_i\}, \\ \mathbf{H}^s, & \text{in } \mathbb{R}^3 \setminus G_+. \end{cases}$$

The total field satisfies in $\{x_2 < H_i\}$ and the scattered field satisfies in \mathbb{R}^3 the time-harmonic Maxwell equations

$$\nabla \times \mathbf{E} = i\tilde{\omega}\mu \mathbf{H} \quad \text{and} \quad \nabla \times \mathbf{H} = -i\tilde{\omega}\varepsilon \mathbf{E} \quad (2.3)$$

with the modified frequency

$$\tilde{\omega} = \omega \frac{d}{2\pi} = \frac{d}{\lambda \sqrt{\varepsilon_0 \mu_0}},$$

where ε_0, μ_0 are the dielectric constant and the permeability of vacuum, λ denotes the wave length.

The functions ε and μ are discontinuous on certain surfaces $\Lambda \times \mathbb{R}$ between different media. Then the tangential components of the total fields are continuous when crossing this interface

$$[\mathbf{n} \times \mathbf{E}] = 0 \quad \text{and} \quad [\mathbf{n} \times \mathbf{H}] = 0 \quad \text{on } \Lambda \times \mathbb{R}, \quad (2.4)$$

where \mathbf{n} is the unit normal to $\Lambda \times \mathbb{R}$ and $[\cdot]$ denotes the difference between the values on different sides of Λ . Hence, at the boundary ∂G_+ of the semi-infinite domain G_+ above the periodic structure the transmission condition has the form

$$\mathbf{n} \times (\mathbf{E}^{inc} + \mathbf{E}^s)|_{\partial G_+}^+ = \mathbf{n} \times \mathbf{E}^s|_{\partial G_+}^- \quad \text{and} \quad \mathbf{n} \times (\mathbf{H}^{inc} + \mathbf{H}^s)|_{\partial G_+}^+ = \mathbf{n} \times \mathbf{H}^s|_{\partial G_+}^-, \quad (2.5)$$

where $u|_{\partial G_+}^\pm$ denote the boundary values of the function u from above resp. below at the surface ∂G_+

2.2 Floquet-Fourier Transform

For a function $f(x_1, x_2, x_3)$ in \mathbb{R}^3 the Floquet-Fourier transformation is defined as

$$\begin{aligned} \mathcal{U}f(x_1, x_2, \xi_3; \xi_1) &= \sum_{m=-\infty}^{\infty} e^{2\pi i m \xi_1} \int_{-\infty}^{\infty} f(x_1 - 2\pi m, x_2, x_3) e^{i x_3 \xi_3} dx_3 \\ &= \sum_{m=-\infty}^{\infty} e^{2\pi i m \xi_1} \mathcal{F}_3 f(x_1 - 2\pi m, x_2, \xi_3), \end{aligned} \quad (2.6)$$

where $\mathcal{F}_3 f$ denotes the Fourier transform of f with respect to the variable x_3 . This combination of Floquet transform with respect to x_1 and Fourier transform with respect to x_3 has the following properties:

- The application of Poisson's summation formula gives the equivalent representation

$$\mathcal{U}f(x_1, x_2, \xi_3; \xi_1) = \frac{1}{2\pi} \sum_{m=-\infty}^{\infty} \mathcal{F}_{13}f(m - \xi_1, x_2, \xi_3) e^{-ix_1(m-\xi_1)}, \quad (2.7)$$

where $\mathcal{F}_{13}f = \mathcal{F}_1(\mathcal{F}_3f)$ is the two-dimensional Fourier transform

$$\mathcal{F}_{13}f(\xi_1, x_2, \xi_3) = \int_{\mathbb{R}^2} f(x_1, x_2, x_3) e^{i(x_1\xi_1+x_3\xi_3)} dx_1 dx_3.$$

- ξ_1 -quasiperiodicity in x_1 and 1-periodicity in ξ_1 of the form

$$\begin{aligned} \mathcal{U}f(x_1 + 2\pi, x_2, \xi_3; \xi_1) &= e^{2\pi i \xi_1} \mathcal{U}f(x_1, x_2, \xi_3; \xi_1), \\ \mathcal{U}f(x_1, x_2, \xi_3; \xi_1 + 1) &= \mathcal{U}f(x_1, x_2, \xi_3; \xi_1). \end{aligned}$$

- Inversion formula

$$f(x_1, x_2, x_3) = \frac{1}{2\pi} \int_{-\infty}^{\infty} e^{-ix_3\xi_3} d\xi_3 \int_{-1/2}^{1/2} \mathcal{U}f(x_1, x_2, \xi_3; \xi_1) d\xi_1. \quad (2.8)$$

- Relation for partial derivatives

$$\mathcal{U}(\partial_{x_1}f) = \partial_{x_1}\mathcal{U}f, \quad \mathcal{U}(\partial_{x_2}f) = \partial_{x_2}\mathcal{U}f, \quad \mathcal{U}(\partial_{x_3}f) = -i\xi_3\mathcal{U}f$$

- If $\rho(x_1, x_2)$ is 2π -periodic function in x_1 , then

$$\mathcal{U}(\rho f)(x_1, x_2, \xi_3; \xi_1) = \rho(x_1, x_2)\mathcal{U}f(x_1, x_2, \xi_3; \xi_1).$$

2.3 Transformation of the Maxwell system

In the following we apply the transform (2.6) to the Maxwell problem (2.3). This results in the partial differential system for the vector functions $\mathcal{U}\mathbf{E}^s(\xi_1; x_1, x_2, \xi_3)$ and $\mathcal{U}\mathbf{H}^s(\xi_1; x_1, x_2, \xi_3)$

$$\mathcal{U}(\nabla \times \mathbf{E}^s) = \tilde{\nabla} \times \mathcal{U}\mathbf{E}^s = \tilde{\mu}\mathcal{U}\mathbf{H}^s, \quad \mathcal{U}(\nabla \times \mathbf{H}^s) = \tilde{\nabla} \times \mathcal{U}\mathbf{H}^s = -i\tilde{\varepsilon}\mathcal{U}\mathbf{E}^s \quad (2.9)$$

with $\tilde{\nabla} = (\partial_{x_1}, \partial_{x_2}, -i\xi_3)$, where we use the notation

$$\tilde{\varepsilon} = \tilde{\omega}\varepsilon = \frac{d\varepsilon}{\lambda\sqrt{\varepsilon_0\mu_0}} = \frac{d\varepsilon}{\lambda\varepsilon_0} \sqrt{\frac{\varepsilon_0}{\mu_0}}, \quad \tilde{\mu} = \tilde{\omega}\mu = \frac{d\mu}{\lambda\sqrt{\varepsilon_0\mu_0}} = \frac{d\mu}{\lambda\mu_0} \sqrt{\frac{\mu_0}{\varepsilon_0}},$$

and the periodicity of these piecewise constant functions. Moreover, since the normal to any surface $\Lambda \times \mathbb{R}$ does not depend on x_3 , $\mathbf{n} = \mathbf{n}(x_1, x_2)$, and is 2π -periodic in x_1 , the conditions on the interfaces (2.4) and (2.5) transform to

$$\begin{aligned} \mathbf{n} \times (\mathcal{U}\mathbf{E}^{inc} + \mathcal{U}\mathbf{E}^s)|_{\partial G_+}^+ &= \mathbf{n} \times \mathcal{U}\mathbf{E}^s|_{\partial G_+}^-, \quad \mathbf{n} \times (\mathcal{U}\mathbf{H}^{inc} + \mathcal{U}\mathbf{H}^s)|_{\partial G_+}^+ = \mathbf{n} \times \mathcal{U}\mathbf{H}^s|_{\partial G_+}^-, \\ [\mathbf{n} \times \mathcal{U}\mathbf{E}^s] &= 0 \quad \text{and} \quad [\mathbf{n} \times \mathcal{U}\mathbf{H}^s] = 0 \quad \text{on all other interfaces } \Lambda \times \mathbb{R}. \end{aligned} \quad (2.10)$$

We can determine $\mathcal{U}\mathbf{E}^{inc}$ and $\mathcal{U}\mathbf{H}^{inc}$ using the representations (2.1) and (2.2). From Weyl's representation formula of a spherical wave

$$\frac{e^{ik|\mathbf{x}|}}{|\mathbf{x}|} = \frac{i}{2\pi} \int_{\mathbb{R}^2} \frac{e^{i\sqrt{k^2 - \xi_1^2 - \xi_3^2} |x_2|}}{\sqrt{k^2 - \xi_1^2 - \xi_3^2}} e^{i(x_1 \xi_1 + x_3 \xi_3)} d\xi_1 d\xi_3$$

we get for any convolution integral

$$F(\mathbf{x}) = \int_{\mathbb{R}^2} \frac{e^{ik|\mathbf{x}-\mathbf{X}'|}}{|\mathbf{x}-\mathbf{X}'|} f(\mathbf{X}') d\mathbf{X}'$$

the relation

$$\mathcal{F}_{13}F(\xi_1, x_2, \xi_3) = \mathcal{F}_{13}\left(\frac{e^{ik|\cdot|}}{|\cdot|}\right)(\xi_1, x_2, \xi_3) \mathcal{F}_{13}f(\xi_1, \xi_3) = 2\pi i \frac{e^{i\sqrt{k^2 - \xi_1^2 - \xi_3^2} |x_2|}}{\sqrt{k^2 - \xi_1^2 - \xi_3^2}} \mathcal{F}_{13}f(\xi_1, \xi_3).$$

Thus, the representation (2.1) of the incident field \mathbf{E}^{inc} and (2.7) give for $x_2 < H_i$

$$\mathcal{U}\mathbf{E}^{inc}(x_1, x_2, \xi_3; \xi_1) = \frac{1}{2\pi i} \tilde{\nabla} \times \sum_{m=-\infty}^{\infty} e^{-ix_1(m-\xi_1)} \frac{e^{i\sqrt{\kappa_+^2 - (\xi_1-m)^2 - \xi_3^2} (H_i - x_2)}}{\sqrt{\kappa_+^2 - (\xi_1-m)^2 - \xi_3^2}} \mathcal{F}_{13}\mathbf{F}(m - \xi_1, \xi_3).$$

Denoting $\beta_m^+ = \sqrt{\kappa_+^2 - (\xi_1 - m)^2 - \xi_3^2}$, the Floquet-Fourier transform of \mathbf{E}^{inc} is given by the series of quasiperiodic functions

$$\mathcal{U}\mathbf{E}^{inc}(x_1, x_2, \xi_3; \xi_1) = \frac{1}{2\pi} \sum_{m=-\infty}^{\infty} \frac{e^{ix_1(\xi_1-m) + i\beta_m^+ (H_i - x_2)}}{\beta_m^+} \Phi_m \times \mathcal{F}_{13}\mathbf{F}(m - \xi_1, \xi_3) \quad (2.11)$$

with the vectors $\Phi_m = (\xi_1 - m, -\beta_m^+, -\xi_3)^T$ and $\mathcal{F}_{13}\mathbf{F} = (\mathcal{F}_{13}F_1, 0, \mathcal{F}_{13}F_3)^T$. Analogously, (2.2) leads the series representation

$$\mathcal{U}\mathbf{H}^{inc}(x_1, x_2, \xi_3; \xi_1) = \frac{1}{2\pi\tilde{\mu}_+} \sum_{m=-\infty}^{\infty} \frac{e^{ix_1(\xi_1-m) + i\beta_m^+ (H_i - x_2)}}{\beta_m^+} \Phi_m \times \Phi_m \times \mathcal{F}_{13}\mathbf{F}(m - \xi_1, \xi_3). \quad (2.12)$$

In the following we assume that these series converge for almost all $(\xi_1, \xi_3) \in [-1/2, 1/2] \times \mathbb{R}$.

We see, that the Floquet-Fourier transformation converts the 3d Maxwell system to a two-parameter family of 2d quasiperiodic partial differential problems. For given parameters (ξ_1, ξ_3) a ξ_1 -quasiperiodic solution $\mathcal{U}\mathbf{E}^s, \mathcal{U}\mathbf{H}^s$ of the partial differential system (2.9) in \mathbb{R}^2 is sought, which fulfills the conditions on the interfaces (2.10). The data $\mathcal{U}\mathbf{E}^{inc}, \mathcal{U}\mathbf{H}^{inc}$ are bounded and ξ_1 -quasiperiodic, which implies that the solution should be bounded outside the layer $\{(x_1, x_2, x_3) : |x_2| < H\}$, i.e., it can be expanded in Rayleigh series

$$\begin{aligned} \mathcal{U}\mathbf{E}^s(x_1, x_2, \xi_3; \xi_1) &= \sum_{m=-\infty}^{\infty} \mathbf{E}_m^\pm(\xi_1, \xi_3) e^{ix_1(\xi_1-m) \pm i\beta_m^\pm x_2}, \\ \mathcal{U}\mathbf{H}^s(x_1, x_2, \xi_3; \xi_1) &= \sum_{m=-\infty}^{\infty} \mathbf{H}_m^\pm(\xi_1, \xi_3) e^{ix_1(\xi_1-m) \pm i\beta_m^\pm x_2}, \end{aligned} \quad (2.13)$$

for $x_2 \gtrless \pm H$, where $\beta_m^- = \sqrt{\kappa_-^2 - (\xi_1 - m)^2 - \xi_3^2}$ and the vectors $\mathbf{E}_m^\pm(\xi_1, \xi_3), \mathbf{H}_m^\pm(\xi_1, \xi_3) \in \mathbb{C}^3$.

In view of the inversion formula (2.8) the scattered field $(\mathbf{E}^s, \mathbf{H}^s)$ can be obtained from the integrals

$$\begin{aligned}\mathbf{E}^s(x_1, x_2, x_3) &= \frac{1}{2\pi} \int_{-\infty}^{\infty} e^{-ix_3\xi_3} d\xi_3 \int_{-1/2}^{1/2} \mathcal{U}\mathbf{E}^s(x_1, x_2, \xi_3; \xi_1) d\xi_1, \\ \mathbf{H}^s(x_1, x_2, x_3) &= \frac{1}{2\pi} \int_{-\infty}^{\infty} e^{-ix_3\xi_3} d\xi_3 \int_{-1/2}^{1/2} \mathcal{U}\mathbf{H}^s(x_1, x_2, \xi_3; \xi_1) d\xi_1,\end{aligned}\tag{2.14}$$

where for almost all $(\xi_1, \xi_3) \in [-1/2, 1/2] \times \mathbb{R}$ the functions $\mathcal{U}\mathbf{E}^s, \mathcal{U}\mathbf{H}^s$ satisfy the equations (2.9), (2.10) with (2.11), (2.12) and the radiation condition (2.13).

2.4 Comparison with conical diffraction

Equations (2.9), (2.10) are known from the so-called conical diffraction, modeling the scattering of a plane wave with oblique incidence by the given grating. Indeed, taking spherical coordinates $x_1 = \sin \theta \cos \phi$, $x_2 = \cos \theta \cos \phi$, $x_3 = \sin \phi$, $\phi \in [0, \pi]$, and suppose that the grating is illuminated by a plane wave $(\mathbf{E}^i, \mathbf{B}^i) = (p, q) e^{i\kappa_+ \cdot \mathbf{x}}$ with $p, q \in C^3$ and the wave vector $\kappa_+ = \kappa_+(\sin \theta \cos \phi, -\cos \theta \cos \phi, \sin \phi)$, $|\theta| < \pi/2$ and $\phi \in [0, \pi/2)$. This corresponds to oblique incidence of the wave illuminating the grating from above. Setting $\xi_1 = \kappa_+ \sin \theta \cos \phi$ and $\xi_3 = -\kappa_+ \sin \phi$ we rewrite $(\mathbf{E}^i, \mathbf{B}^i) = (p, q) e^{i(\xi_1 x_1 - \beta x_2 - \xi_3 x_3)}$ with $\beta^2 = \sqrt{\kappa_+^2 - \xi_1^2 - \xi_3^2}$. Then the ansatz

$$\mathbf{E} = \mathcal{E}(x_1, x_2) e^{-i\xi_3 x_3}, \quad \mathbf{H} = \mathcal{H}(x_1, x_2) e^{-i\xi_3 x_3}$$

with vector functions $\mathcal{E}, \mathcal{H} : \mathbb{R}^2 \rightarrow \mathbb{C}^3$ transforms the Maxwell system (2.3) to the equations

$$\tilde{\nabla} \times \mathcal{E}^s = \tilde{\mu}, \quad \tilde{\nabla} \times \mathcal{H}^s = -i\tilde{\varepsilon} \mathcal{E}^s\tag{2.15}$$

for the scattered fields $\mathcal{E}^s, \mathcal{H}^s$ subject to the transmission conditions

$$\begin{aligned}\mathbf{n} \times (\mathcal{E}^i + \mathcal{E}^s)|_{\partial G_+}^+ &= \mathbf{n} \times \mathcal{E}^s|_{\partial G_+}^-, \quad \mathbf{n} \times (\mathcal{H}^i + \mathcal{H}^s)|_{\partial G_+}^+ = \mathbf{n} \times \mathcal{H}^s|_{\partial G_+}^-, \\ [\mathbf{n} \times \mathcal{E}^s] &= 0 \quad \text{and} \quad [\mathbf{n} \times \mathcal{H}^s] = 0 \quad \text{on all other interfaces} \quad \Lambda \times \mathbb{R}\end{aligned}\tag{2.16}$$

with the incident plane wave $(\mathcal{E}^i, \mathcal{H}^i) = (p, q) e^{i(\xi_1 x_1 - \beta x_2)}$. Besides, $\mathcal{E}^s, \mathcal{H}^s$ have to satisfy the radiation condition (2.13).

There exist different approaches to the numerical solution of off-plane diffraction, (cf. [11]), either based on the solution of the Maxwell system in \mathbb{R}^3 , of the system (2.15) in \mathbb{R}^2 or on the solution of a system of two Helmholtz equations. The last one is based on the fact that the components of $\mathcal{E}^s, \mathcal{H}^s$ are solutions of

$$\Delta u + (\kappa^2 - \xi_3^2)u = 0, \quad (x_1, x_2) \in \mathbb{R}^2,\tag{2.17}$$

with the piecewise constant coefficients $\kappa^2 - \xi_3^2$. Moreover, if $\kappa^2 - \xi_3^2 \neq 0$, than 2 of the 6 components are sufficient to determine the solution (\mathbf{E}, \mathbf{H}) of the quasiperiodic Maxwell system (2.3), and these two components are coupled by special transmission conditions on the interfaces between different media. For example, if one chooses the third components $\mathcal{E}_3^s, \mathcal{H}_3^s$ and denotes $\mathcal{B}_3^s = \sqrt{\mu_0/\varepsilon_0} \mathcal{H}_3^s$, then on the upper interface $D_+ = G_+ \cap \mathbb{R}^2$ the jump conditions read as

$$\begin{aligned}(\mathcal{E}_3^s + \mathcal{E}_3^i)|_{\partial D_+}^+ &= \mathcal{E}_3^s|_{\partial D_+}^-, \quad \frac{\tilde{\varepsilon} \partial_n (\mathcal{E}_3^s + \mathcal{E}_3^i) - \xi_3 \partial_t (\mathcal{B}_3^s + \mathcal{B}_3^i)}{\kappa^2 - \xi_3^2} \Big|_{\partial D_+}^+ = \frac{\tilde{\varepsilon} \partial_n \mathcal{E}_3^s - \xi_3 \partial_t \mathcal{B}_3^s}{\kappa^2 - \xi_3^2} \Big|_{\partial D_+}^-, \\ (\mathcal{B}_3^s + \mathcal{B}_3^i)|_{\partial D_+}^+ &= \mathcal{B}_3^s|_{\partial D_+}^-, \quad \frac{\tilde{\mu} \partial_n (\mathcal{B}_3^s + \mathcal{B}_3^i) + \xi_3 \partial_t (\mathcal{E}_3^s + \mathcal{E}_3^i)}{\kappa^2 - \xi_3^2} \Big|_{\partial D_+}^+ = \frac{\tilde{\mu} \partial_n \mathcal{B}_3^s + \xi_3 \partial_t \mathcal{E}_3^s}{\kappa^2 - \xi_3^2} \Big|_{\partial D_+}^-\end{aligned}\tag{2.18}$$

with $\mathcal{E}_3^i = p_3 e^{i(\xi_1 x_1 - \beta x_2)}$, $\mathcal{B}_3^i = q_3 \sqrt{\mu_0/\varepsilon_0} e^{i(\xi_1 x_1 - \beta x_2)}$, and on all other interfaces Λ

$$[\mathcal{E}_3^s] = [\mathcal{B}_3^s] = 0, \left[\frac{\tilde{\varepsilon} \partial_n \mathcal{E}_3^s - \xi_3 \partial_t \mathcal{B}_3^s}{\kappa^2 - \xi_3^2} \right]_{\Lambda} = \left[\frac{\tilde{\mu} \partial_n \mathcal{B}_3^s + \xi_3 \partial_t \mathcal{E}_3^s}{\kappa^2 - \xi_3^2} \right]_{\Lambda} = 0. \quad (2.19)$$

This transmission problem (2.17), (2.18), (2.19) for \mathcal{E}_3^s , \mathcal{B}_3^s together with the radiation condition (2.13) was used for the mathematical analysis of conical diffraction by studying equivalent variational equations or systems of integral equations over the interfaces. Besides conditions on the existence and uniqueness of solutions also stability and convergence results for finite element and boundary element methods have been obtained, cf. [5], [14].

Existing solvers for conical diffraction can easily be adapted to the solution of the Floquet-Fourier transformed Maxwell problems, since the only difference to conical diffraction is the appearance of $\mathcal{U}\mathbf{E}^{inc}$, $\mathcal{U}\mathbf{H}^{inc}$ as sum of ξ_1 -quasiperiodic plane waves instead of the single ξ_1 -quasiperiodic plane wave \mathcal{E}^i , \mathcal{U}^i . The numerical results listed below have been obtained by an efficient integral method, which is based on the solution of a 2×2 system of singular integral equations on each interface ([8], [9], [15], [13]).

3 Field computation

For given parameters (ξ_1, ξ_3) the square root $\beta_m^\pm = \sqrt{\kappa_\pm^2 - \xi_3^2 - (\xi_1 - m)^2}$ is real only for integers m belonging to finite sets $\Sigma_\pm(\xi_1, \xi_3)$, which give raise to propagating reflected or transmitted modes. In all other cases $\text{Im} \sqrt{\kappa_\pm^2 - \xi_3^2 - (\xi_1 - m)^2} > 0$, such that the remaining terms

$$\sum_{m \notin \Sigma_\pm(\xi_1, \xi_3)} (\mathbf{E}_m^\pm(\xi_1, \xi_3), \mathbf{H}_m^\pm(\xi_1, \xi_3)) e^{i(\xi_1 - m)x_1 \pm i \sqrt{\kappa_\pm^2 - \xi_3^2 - (\xi_1 - m)^2} x_2}, \quad (3.1)$$

form evanescent fields, concentrated in the vicinity of the boundary of the periodic structure. Since we are interested to compute the scattered fields outside the layer $\{(x_1, x_2, x_3) : |x_2| < H\}$, for any point (x_1, x_2) , $\pm x_2 \geq H$, the solution $\mathcal{U}\mathbf{E}^s, \mathcal{U}\mathbf{H}^s$ is approximated with high accuracy by a finite sum

$$(\mathcal{U}\mathbf{E}^s, \mathcal{U}\mathbf{H}^s)(x_1, x_2, \xi_3; \xi_1) \approx \sum_{m \in \tilde{\Sigma}_\pm(\xi_1, \xi_3)} (\mathbf{E}_m^\pm(\xi_1, \xi_3), \mathbf{H}_m^\pm(\xi_1, \xi_3)) e^{ix_1(\xi_1 - m) \pm i\beta_m^\pm x_2}, \quad (3.2)$$

where $\tilde{\Sigma}_\pm(\xi_1, \xi_3) \supseteq \Sigma_\pm(\xi_1, \xi_3)$ may contain integer values m associated with evanescent modes. Then the scattered field is approximated for $|x_2| > H$ using a cubature of the integrals (2.14)

$$\begin{aligned} \mathbf{E}^s(x_1, x_2, x_3) &\approx \frac{1}{2\pi} \sum_{j=1}^N \omega_j \mathcal{U}\mathbf{E}^s(x_1, x_2, \xi_3^{(j)}; \xi_1^{(j)}) e^{-ix_3 \xi_3^{(j)}}, \\ \mathbf{H}^s(x_1, x_2, x_3) &\approx \frac{1}{2\pi} \sum_{j=1}^N \omega_j \mathcal{U}\mathbf{H}^s(x_1, x_2, \xi_3^{(j)}; \xi_1^{(j)}) e^{-ix_3 \xi_3^{(j)}}. \end{aligned} \quad (3.3)$$

Here ω_n and $(\xi_1^{(j)}, \xi_3^{(j)}) \in (1/2, 1/2] \times \mathbb{R}$ are the weights and positions of cubature knots, respectively.

3.1 Splitting of the integration domain

However, a simple application of 2d-cubature formulas (3.3) may lead to doubtful results or to inappropriate computational costs. This is caused by the non-smoothness or irregular behavior of $\mathcal{U}\mathbf{E}^s$, $\mathcal{U}\mathbf{H}^s$ as functions of (ξ_1, ξ_3) , which can have several reasons.

We mention first, that the terms $e^{i\beta_m^\pm |x_2|} = e^{i\sqrt{\kappa_\pm^2 - \xi_3^2 - (\xi_1 - m)^2} |x_2|}$ appearing in (3.3) are not smooth near the Rayleigh frequencies, the zeros of the curves $\kappa_\pm^2 - \xi_3^2 - (\xi_1 - m)^2 = 0$ for $m \in \mathbb{Z}$, $|m| \leq [\kappa_\pm]$, where $[k]$ denotes the integer part of $k > 0$. Besides the singularity of the square root the number of propagating modes changes near these curves, since the integer m is associated with a propagating mode if $\kappa_\pm^2 - \xi_3^2 - (\xi_1 - m)^2 \geq 0$ and with an exponentially decaying evanescent mode for $\kappa_\pm^2 - \xi_3^2 - (\xi_1 - m)^2 < 0$.

Simple tests show that it necessary to split the integration domain $(0, 1) \times \mathbb{R}$ of the integrals (2.14) into subdomains where the number of propagating modes is constant, i.e. the subdomains are bounded by the curves $\xi_3 = \pm\sqrt{\kappa_\pm^2 - (\xi_1 - m)^2}$ for $m \in \mathbb{Z}$, $|m| \leq [\kappa_\pm]$. In Figure 1 the splitting is shown for $\kappa = 3.4$ and $\xi_3 \geq 0$, which must be extended symmetrically to $\xi_3 < 0$. Since $\mathcal{U}\mathbf{E}^s$, $\mathcal{U}\mathbf{H}^s$ are 1-periodic in ξ_1 , the splitting can be performed such, that it consists of 2 infinite domains $\{\xi_1 \in (-1/2, 1/2), |\xi_3| > \sqrt{\kappa_\pm^2 - \xi_1^2}\}$ and a finite number of closed curved polygons, contained either in the strip $-1/2 \leq \xi_1 \leq 1/2$ or in the strip $0 \leq \xi_1 \leq 1$. This is depicted in Figure 2, also for $\xi_3 \geq 0$.

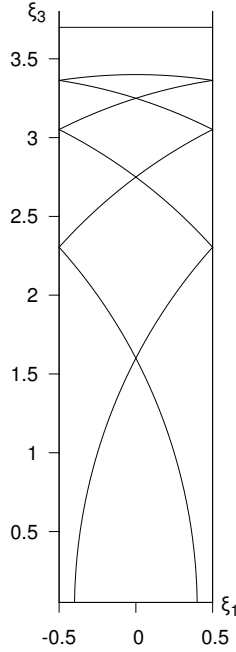


Figure 1: Splitting of the integration domain for $\xi_3 \geq 0$

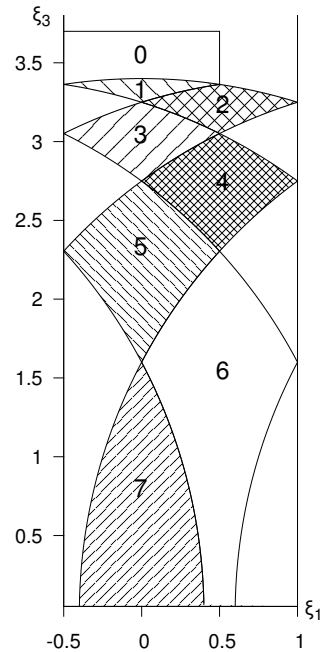


Figure 2: Splitting into closed curved polygons for $\xi_3 \geq 0$, the numbers of propagating modes are indicated in each subdomain

3.2 Behavior of Rayleigh coefficients

Inside the subdomains with a constant number of propagating modes the Rayleigh coefficients $\mathbf{E}_m^\pm = \mathbf{E}_m^\pm(\xi_1, \xi_3)$ and $\mathbf{H}_m^\pm = \mathbf{H}_m^\pm(\xi_1, \xi_3)$ can behave non-smoothly or fast oscillating. But in contrast to the problem with the Rayleigh frequencies, which satisfy $\kappa_\pm^2 - \xi_3^2 - (\xi_1 - m)^2 = 0$ for some $m \in \mathbb{Z}$, the behavior of the Rayleigh coefficients strongly depends on the illuminating field, the geometry and the materials of the periodic structure. In the following we illustrate the dependence of the Rayleigh coefficients \mathbf{E}_m^-

on the incident field for the simple case of classical diffraction, when the illuminating beam is independent on x_3 .

We consider a binary grating of fused silica with period 800 nm, depth 400 nm and fill factor 0.5. It is illuminated by a 2d-Gaussian beam, by a plane wave with normal incidence through a slit and by a wave emitted by a line source, all having the wave length 880 nm. In this case, the grating transmits 3 outgoing waves if $|\xi_1| < 0.32$, and 2 outgoing waves for $0.32 < |\xi_1| < 0.5$. In Fig. 3 we plot the imaginary parts of the third components of $\mathbf{H}_m^-(\xi_1, 0)$. For $|\xi_1| < 0.32$ we set $f(m + \xi_1) = \text{Im}(\mathbf{H}_m^-)_3(\xi_1, 0)$ for the three orders $m = 0, \pm 1$. The gap in the argument $0.32 < \xi_1 < 0.68$ is filled with the values $f(m + \xi_1) = \text{Im}(\mathbf{H}_m^-)_3(\xi_1, 0)$ for the two orders $m = 0, -1$.

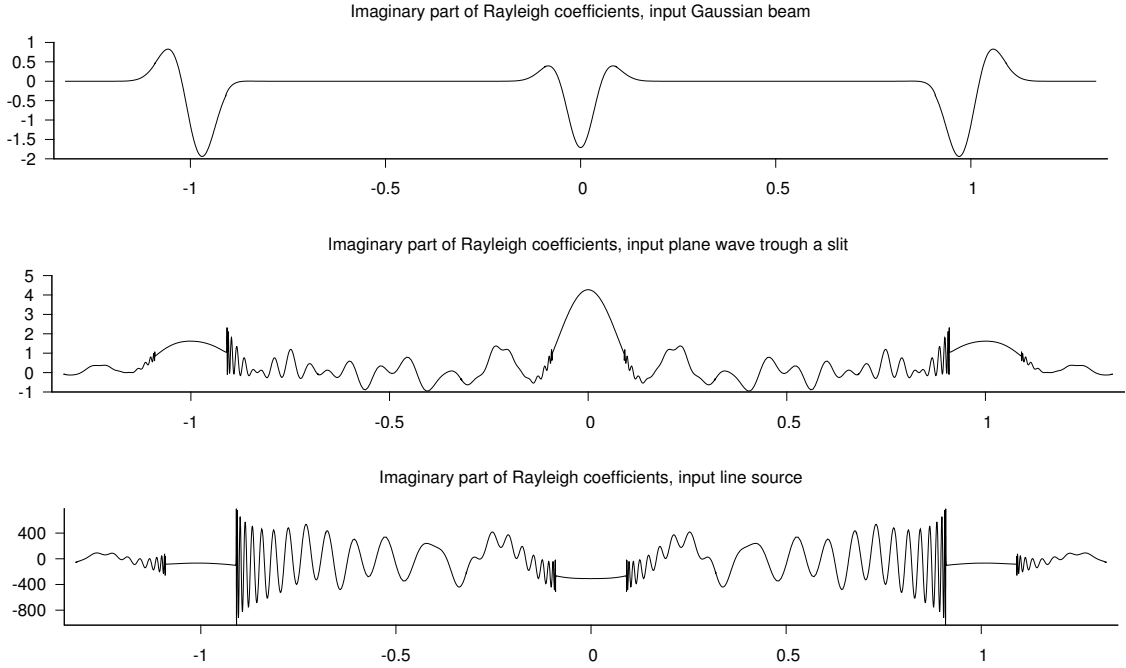


Figure 3: Plot of the imaginary parts of $f(m + \xi_1) = (\mathbf{H}_m^-)_3(\xi_1, 0)$, $|\xi_1| \leq 0.32$, $|m| \leq 1$.

It is interesting that oscillations or even jumps of the Rayleigh coefficients can occur at Rayleigh frequencies for reflection, which appear at $\xi_1 \approx 0.09$. The grating is illuminated from air, the incidence of plane waves $e^{i(\xi_1 x_1 - \beta^+ x_2)}$ leads to one reflection mode if $|\xi_1| < 0.09$ and otherwise to two reflection modes. Other numerical experiments with gratings with more than 2 materials indicate, that in general irregular behavior of Rayleigh coefficients can occur for points (ξ_1, ξ_3) , when for some material parameter κ of the grating $\kappa^2 - \xi_3^2 - (\xi_1 - m)^2 = 0$ with integer m . Hence a further subdivision of the integration domain could be useful. In the case of classical diffraction the implementation can be carried out rather easily, whereas in the case of 3d-illumination a further subdivision of the integration domain leads to in general rather complicated situations with a large number of subdomains.

3.3 Cubature of 2d-integrals

In order to develop efficient cubature formulas (3.3) a better theoretical understanding of the dependence of Rayleigh coefficients on incidence angles and their behavior is necessary, but not available. In the case of 3d-illumination we restrict to the subdivision of the integration domain indicated in Fig. 2 and try to apply

an approach able to control the accuracy of the calculated scattered fields. The integrals over the curved polygons can easily be transformed into integrals over squares or triangles, for which different cubature formulas can be found in the literature.

But one should mention that the construction of high-quality approximation rules even for 2d-integrals still remains a current research problem, cf. [6], [10], [7]. There exists no unique best criterion for the choice of weights and points in the integral approximation. The generally accepted rule is that this choice should provide the exact integration for a class of integrands in the form of polynomials of a certain algebraic degree. In particular, the N -point Gaussian quadrature is exact for all one-dimensional polynomials of degree at most $P = 2N - 1$. Analogously, in the case of two variables it is necessary to construct an N -point cubature scheme which would be perfect for all two-dimensional polynomials with the maximal total degree P . In order that cubature rule is efficient, the number N of points should be as small as possible for each given value P . But up to now, the lowest possible number N_{min} of points (knots) is unknown, in general. Moreover, the nonlinear equations, which appear when constructing the cubature rule of a high degree P , become too complicated to be analyzed theoretically, and the only way is to solve them numerically. However, the straightforward scheme, based on the product of two Gaussian quadratures to get a cubature formula, is very inefficient for large degree P . Since the function evaluation at a cubature knot (ξ_1, ξ_3) in (3.3) requires the solution of a conical diffraction problem, we don't use tensor products of 1d-formulas, but try to apply an efficient 2d-cubature rule.

Concerning adaptive cubature algorithms for 2d-integrals the situation is similar restricted when compared to the case of 1d-integrals, where different adaptive integration methods are known. There exist only few cubature algorithms for rectangles, which is the most suited for our problem, and they are closely related [4], [1], [2]. After some testing we implemented an algorithm mainly based on ideas of the Cuhre algorithm described in [2]. The algorithm uses integration rules of polynomial degree 7, 9, and 13 and a globally adaptive subdivision strategy. In each iteration, the subregion with the largest estimated error is halved along the axis where the integrand has the largest fourth divided difference. The a posteriori error estimates produced by the algorithm use approximations by null rules, which are calculated simultaneously with the integration rule. Details on the algorithm can be found in the original references [2] and on the employed cubature rules in the Cuba library [12], which provides an implementation of Cuhre and three other cubature algorithms based on Monte Carlo integration.

3.4 Description of the algorithm

The aim of the algorithm is to compute an approximation of the scattered fields for a given finite point set S outside the layer $\{(x_1, x_2, x_3) : |x_2| < H\}$ with a prescribed absolute or relative error. This can be done using an adaptive method based on reliable error estimations. Our realization of the adaptive approach extends some modules provided by [12], where we have to take into account that at a cubature knot $(\xi_1^{(j)}, \xi_3^{(j)})$ the evaluation of the coefficients $\mathbf{E}_m^\pm(\xi_1^{(j)}, \xi_3^{(j)})$, $\mathbf{H}_m^\pm(\xi_1^{(j)}, \xi_3^{(j)})$ in (3.2) for $m \in \tilde{\Sigma}_\pm(\xi_1^{(j)}, \xi_3^{(j)})$ corresponds to the solution of a transmission problem (2.9), (2.10) with $\mathcal{U}\mathbf{E}^{inc}(x_1, x_2, \xi_3^{(j)}; \xi_1^{(j)})$ and $\mathcal{U}\mathbf{H}^{inc}(x_1, x_2, \xi_3^{(j)}; \xi_1^{(j)})$ given by (2.11), (2.12).

Let us mention, that besides the control of the accuracy of the scattered field calculations the adaptive method has the advantage, that it determines automatically the nodes $(\xi_1^{(j)}, \xi_3^{(j)})$ for the discrete approximation of the incident functions $\mathcal{U}\mathbf{E}^{inc}$ and $\mathcal{U}\mathbf{H}^{inc}$. This is based on the a posteriori error estimations of the scattered field and no further knowledge of the incident functions is required. Hence the incident functions $\mathcal{U}\mathbf{E}^{inc}$ and $\mathcal{U}\mathbf{H}^{inc}$ are expanded into quasiperiodic wave functions $\mathcal{U}\mathbf{E}^{inc}(x_1, x_2, \xi_3^{(j)}; \xi_1^{(j)})$ and $\mathcal{U}\mathbf{H}^{inc}(x_1, x_2, \xi_3^{(j)}; \xi_1^{(j)})$ such that the resulting scattered field approximations are "optimal". This feature together with the computation of incident functions $\mathcal{U}\mathbf{E}^{inc}$ and $\mathcal{U}\mathbf{H}^{inc}$ seems to be characteristic for our

approach.

First the integration domain is split into subdomains Ω_k with the same number of propagating modes k , as indicated in Fig. 2. Then the integrals (2.14) are the sums over the subdomains

$$\mathbf{E}^s(x_1, x_2, x_3) = \frac{1}{2\pi} \sum_{k=0}^N \iint_{\Omega_k} \mathcal{U}\mathbf{E}^s(x_1, x_2, \xi_3; \xi_1) e^{-ix_3\xi_3} d\xi_1 d\xi_3,$$

$$\mathbf{H}^s(x_1, x_2, x_3) = \frac{1}{2\pi} \sum_{k=0}^N \iint_{\Omega_k} \mathcal{U}\mathbf{H}^s(x_1, x_2, \xi_3; \xi_1) e^{-ix_3\xi_3} d\xi_1 d\xi_3,$$

where N is the maximal order of propagating modes. For each Ω_k we specify index sets $\tilde{\Sigma}_{\pm}(k)$, containing indices of all propagating and possibly of some evanescent modes. Note that the domains Ω_0 correspond to the unbounded subdomains of the integration domain with $|\xi_3| > \sqrt{\kappa_{\pm}^2 - \xi_1^2}$ for $|\xi_1| \leq 1/2$. The integrals gives only an exponentially decaying contribution to the scattered fields, so in most cases they can be neglected. If otherwise $\tilde{\Sigma}_{\pm}(0) \neq \emptyset$, then we truncate Ω_0 to bounded sets with $\sqrt{\kappa_{\pm}^2 - \xi_1^2} < |\xi_3| < c\kappa_{\pm}$ with a constant $c > 1$.

As mentioned above, the subdomains Ω_k (or parts of it) can easily be presented as the image of continuous mappings of reference integration domains, the unit square or a triangle. For simplicity, in the following we will describe the adaptive algorithm in the simple case that $\Omega_k = \chi_k(\square)$, where \square is the unit square and χ_k denotes the continuous transformation. This applies analogously to the cases, that Ω_k is the image of a triangle or represents the union of images of squares or triangles.

3.4.1 Adaptive algorithm

After subdivision the adaptive algorithm is applied to each $\Omega_k = \chi_k(\square)$ separately. The formal description of the procedure coincides with the general structure of adaptive algorithms for numerical integration:

- (i) Choose the subregion with the largest local error from a set of subregions.
- (ii) Subdivide the chosen subregion into two subregions.
- (iii) Perform the cubature and error estimation for the new subregions; update the subregion set.
- (iv) Update error estimates; check for convergence.

Topics (ii)-(iv) need some explanation.

(ii): The subdomains are of the form $\chi_k(R)$ for a rectangle $R \subset \square$ with sides parallel to the coordinate axis. The algorithm bisects R into two rectangles R_1 and R_2 along the coordinate axis where the integrand has largest fourth divided difference, as proposed for the Cuhre algorithm[2]. Then $\chi_k(R)$ is subdivided into $\chi_k(R_1)$, $\chi_k(R_2)$. The computation of the integrand values is explained in the next topic **(iii)**. These values are associated with knots $(\xi_1^{(j)}, \xi_3^{(j)})$, which also appear in the cubature rule for the integrals over $\chi_k(R_1)$, $\chi_k(R_2)$ and can be reused. So the calculation of the differences does not significantly contribute to the computation time.

(iii): From **(ii)** we derive two subregions associated with rectangles R_1 and R_2 , for which the integrals should be approximated. Denoting by R one of the rectangles R_1 and R_2 we explain here how the cubature of the integrals over $\chi_k(R) \subset \Omega_k$ and the error estimation are handled. The algorithm specifies the cubature formula with weights ω_j and knots $(\rho_1^{(j)}, \rho_3^{(j)}) \in R$. The nodes are mapped to parameters $(\xi_1^{(j)}, \xi_3^{(j)}) = \chi_k(\rho_1^{(j)}, \rho_3^{(j)}) \in \chi_k(R)$, for which the diffraction problem (2.9), (2.10) has to be solved. As the first step approximations of $\mathcal{U}\mathbf{E}^{inc}$ and $\mathcal{U}\mathbf{H}^{inc}$ are computed,

$$\begin{aligned}\mathcal{U}\mathbf{E}^{inc}(x_1, x_2, \xi_3^{(j)}; \xi_1^{(j)}) &\approx \frac{1}{2\pi} \sum_{m \in \tilde{\Sigma}_+(k)} \frac{e^{ix_1(\xi_1-m) + i\beta_m^+(H_i-x_2)}}{\beta_m^+} \Phi_m \times \mathcal{F}_{13}\mathbf{F}(m - \xi_1^{(j)}, \xi_3^{(j)}), \\ \mathcal{U}\mathbf{H}^{inc}(x_1, x_2, \xi_3^{(j)}; \xi_1^{(j)}) &\approx \frac{1}{2\pi\tilde{\mu}_+} \sum_{m \in \tilde{\Sigma}_+(k)} \frac{e^{ix_1(\xi_1-m) + i\beta_m^+(H_i-x_2)}}{\beta_m^+} \Phi_m \times \Phi_m \times \mathcal{F}_{13}\mathbf{F}(m - \xi_1^{(j)}, \xi_3^{(j)}),\end{aligned}$$

cf. (2.11), (2.12). Here (x_1, x_2) are points on the upper interface $D_+ = \partial G_+ \cap \mathbb{R}^2$. Since the corresponding diffraction problem is solved with the integral method, only the third components of $\mathcal{U}\mathbf{E}_3^{inc}$ and $\mathcal{U}\mathbf{H}_3^{inc}$ are needed. The integral solver computes the third components $e_m^\pm(\xi_1^{(j)}, \xi_3^{(j)})$, $h_m^\pm(\xi_1^{(j)}, \xi_3^{(j)})$ of the Rayleigh coefficient vectors $\mathbf{E}_m^\pm(\xi_1^{(j)}, \xi_3^{(j)})$ and $\mathbf{H}_m^\pm(\xi_1^{(j)}, \xi_3^{(j)})$ of the solution.

Then for the given finite set S of points $\mathbf{x} = (x_1, x_2, x_3)$ the values

$$\begin{aligned}f_E(\mathbf{x}, \xi_1^{(j)}, \xi_3^{(j)}) &= \frac{e^{-ix_3\xi_3^{(j)}}}{2\pi} \sum_{m \in \tilde{\Sigma}_\pm(k)} e_m^\pm(\xi_1^{(j)}, \xi_3^{(j)}) e^{i(\xi_1^{(j)}-m)x_1 \pm i\sqrt{\kappa_\pm^2 - (\xi_3^{(j)})^2 - (\xi_1^{(j)}-m)^2} x_2}, \\ f_H(\mathbf{x}, \xi_1^{(j)}, \xi_3^{(j)}) &= \frac{e^{-ix_3\xi_3^{(j)}}}{2\pi} \sum_{m \in \tilde{\Sigma}_\pm(k)} h_m^\pm(\xi_1^{(j)}, \xi_3^{(j)}) e^{i(\xi_1^{(j)}-m)x_1 \pm i\sqrt{\kappa_\pm^2 - (\xi_3^{(j)})^2 - (\xi_1^{(j)}-m)^2} x_2},\end{aligned}$$

can be considered as a vector of integrand values at the cubature knots $(\rho_1^{(j)}, \rho_3^{(j)}) \in R$. Note that the computation of the fourth divided difference, mentioned in **(ii)**, is performed with these vectors of integrand values at special cubature knots. As usual, the weighted sums of the integrand values

$$E_R(\mathbf{x}) = \sum_{j=1}^N \omega_j f_E(\mathbf{x}, \xi_1^{(j)}, \xi_3^{(j)}), \quad H_R(\mathbf{x}) = \frac{1}{2\pi} \sum_{j=1}^N \omega_j f_H(\mathbf{x}, \xi_1^{(j)}, \xi_3^{(j)}) \quad (3.4)$$

are approximations of the integrals

$$\frac{1}{2\pi} \iint_{\chi_k(R)} \mathcal{U}\mathbf{E}_3^s(x_1, x_2, \xi_3; \xi_1) e^{-ix_3\xi_3} d\xi_1 d\xi_3, \quad \iint_{\chi_k(R)} \mathcal{U}\mathbf{H}_3^s(x_1, x_2, \xi_3; \xi_1) e^{-ix_3\xi_3} d\xi_1 d\xi_3.$$

Moreover, sums of the form (3.4) with different weights $\omega_j^{(i)}$, $i = 1, \dots, 4$, are the null rules, which are used to compute local estimators of the cubature error for the integrals over $\chi_k(R)$, as described in [2]. The maximum over all $\mathbf{x} \in S$ of these error bounds is taken as the local error on $\chi_k(R)$.

This procedure is done for both rectangles R_1 and R_2 . The subregion set is updated by discarding all values connected with the subdivided rectangle $R_1 \cup R_2$ and by saving the center and sidelength of the rectangles, the cubature results and the local errors, the coefficients $e_m^\pm(\xi_1^{(j)}, \xi_3^{(j)})$, $h_m^\pm(\xi_1^{(j)}, \xi_3^{(j)})$ with the weights $\omega_j^{(i)}$ and parameters $(\xi_1^{(j)}, \xi_3^{(j)})$ for both new subregions R_1 and R_2 for later use.

(iv): If the sum of the local errors for all rectangles of the subdivision exceeds the required error tolerance, then choose the subrectangle R possessing the largest estimated error and go to (ii).

Otherwise, the adaptive procedure is stopped, because for all $\mathbf{x} \in S$ the integrals over Ω_k are calculated with the required accuracy. The integrals over Ω_k are simply the sums of the corresponding saved cubature results for all rectangles in the partition $\Pi(\square)$ of the unit square.

3.4.2 Further field computations

But it is more interesting, that the saved coefficients $e_m^\pm(\xi_1^{(j)}, \xi_3^{(j)})$, $h_m^\pm(\xi_1^{(j)}, \xi_3^{(j)})$, the weights $\omega_j^{(i)}$ and parameters $(\xi_1^{(j)}, \xi_3^{(j)})$ for all rectangles in the partition allow also to calculate approximations of the integrals

$$\frac{1}{2\pi} \iint_{\Omega_k} \mathcal{U}\mathbf{E}_3^s(x_1, x_2, \xi_3; \xi_1) e^{-ix_3\xi_3} d\xi_1 d\xi_3, \quad \iint_{\Omega_k} \mathcal{U}\mathbf{H}_3^s(x_1, x_2, \xi_3; \xi_1) e^{-ix_3\xi_3} d\xi_1 d\xi_3$$

for points $\mathbf{x} \notin S$ outside the layer $\{(x_1, x_2, x_3) : |x_2| < H\}$. For this one has only to use the saved values $e_m^\pm(\xi_1^{(j)}, \xi_3^{(j)})$, $h_m^\pm(\xi_1^{(j)}, \xi_3^{(j)})$, $\omega_j^{(i)}$ and $(\xi_1^{(j)}, \xi_3^{(j)})$ for any rectangle $R \in \Pi(\square)$, to compute

$$E_R(\mathbf{x}) = \frac{1}{2\pi} \sum_{j=1}^N \omega_j e^{-ix_3\xi_3^{(j)}} \sum_{m \in \tilde{\Sigma}_\pm(k)} e_m^\pm(\xi_1^{(j)}, \xi_3^{(j)}) e^{i(\xi_1^{(j)}-m)x_1 \pm i\sqrt{\kappa_\pm^2 - (\xi_3^{(j)})^2 - (\xi_1^{(j)}-m)^2} x_2},$$

$$H_R(\mathbf{x}) = \frac{1}{2\pi} \sum_{j=1}^N \omega_j e^{-ix_3\xi_3^{(j)}} \sum_{m \in \tilde{\Sigma}_\pm(k)} h_m^\pm(\xi_1^{(j)}, \xi_3^{(j)}) e^{i(\xi_1^{(j)}-m)x_1 \pm i\sqrt{\kappa_\pm^2 - (\xi_3^{(j)})^2 - (\xi_1^{(j)}-m)^2} x_2},$$

and to sum

$$\frac{1}{2\pi} \iint_{\Omega_k} \mathcal{U}\mathbf{E}_3^s(x_1, x_2, \xi_3; \xi_1) e^{-ix_3\xi_3} d\xi_1 d\xi_3 \approx \sum_{R \in \Pi(\square)} E_R(\mathbf{x}),$$

$$\frac{1}{2\pi} \iint_{\Omega_k} \mathcal{U}\mathbf{H}_3^s(x_1, x_2, \xi_3; \xi_1) e^{-ix_3\xi_3} d\xi_1 d\xi_3 \approx \sum_{R \in \Pi(\square)} H_R(\mathbf{x}).$$

Since the remaining first and second components of the Rayleigh coefficient vectors $\mathbf{E}_m^\pm(\xi_1^{(j)}, \xi_3^{(j)})$ and $\mathbf{H}_m^\pm(\xi_1^{(j)}, \xi_3^{(j)})$ can be expressed by the third components $e_m^\pm(\xi_1^{(j)}, \xi_3^{(j)})$, $h_m^\pm(\xi_1^{(j)}, \xi_3^{(j)})$ in a simple way, it is straightforward to derive approximations for the integrals

$$\frac{1}{2\pi} \iint_{\Omega_k} \mathcal{U}\mathbf{E}^s(x_1, x_2, \xi_3; \xi_1) e^{-ix_3\xi_3} d\xi_1 d\xi_3, \quad \iint_{\Omega_k} \mathcal{U}\mathbf{H}^s(x_1, x_2, \xi_3; \xi_1) e^{-ix_3\xi_3} d\xi_1 d\xi_3$$

for any point \mathbf{x} outside the layer $\{(x_1, x_2, x_3) : |x_2| < H\}$.

4 Numerical examples

In the final section we present visualizations of the intensities of transmitted fields from a lamellar grating with period $d = 800$ nm, depth $h = 400$ nm and fill factor 0.5 ruled on fused silica. The incident field is supposed to propagate downward from air in the silica region. We consider illumination in normal incidence

by a Gaussian beam, a radially polarized Gaussian beam and a plane wave passing through a small circular aperture.

The pictures show the field intensity in the material below the grating in 4 planes

$$\{(x_1, x_2, x_3) : -20d \leq x_1 \leq 20d, -41d \leq x_2 \leq -d, x_3 = 0\},$$

$$\{(x_1, x_2, x_3) : -20d \leq x_1, x_3 \leq 20d, x_2 = c\}, \quad c = -5d, -10d, -15d.$$

Figure 4 corresponds to the illumination by a Gaussian beam of wave length $\lambda = 880$ nm with normal incidence. The incident \mathbf{E} -field is given by the integral (2.1) with $H_i = 10d$ and the functions

$$F_1(x_1, x_3) = e^{-(x_1^2+x_3^2)/3d}, \quad F_3(x_1, x_3) = i e^{-(x_1^2+x_3^2)/3d}.$$

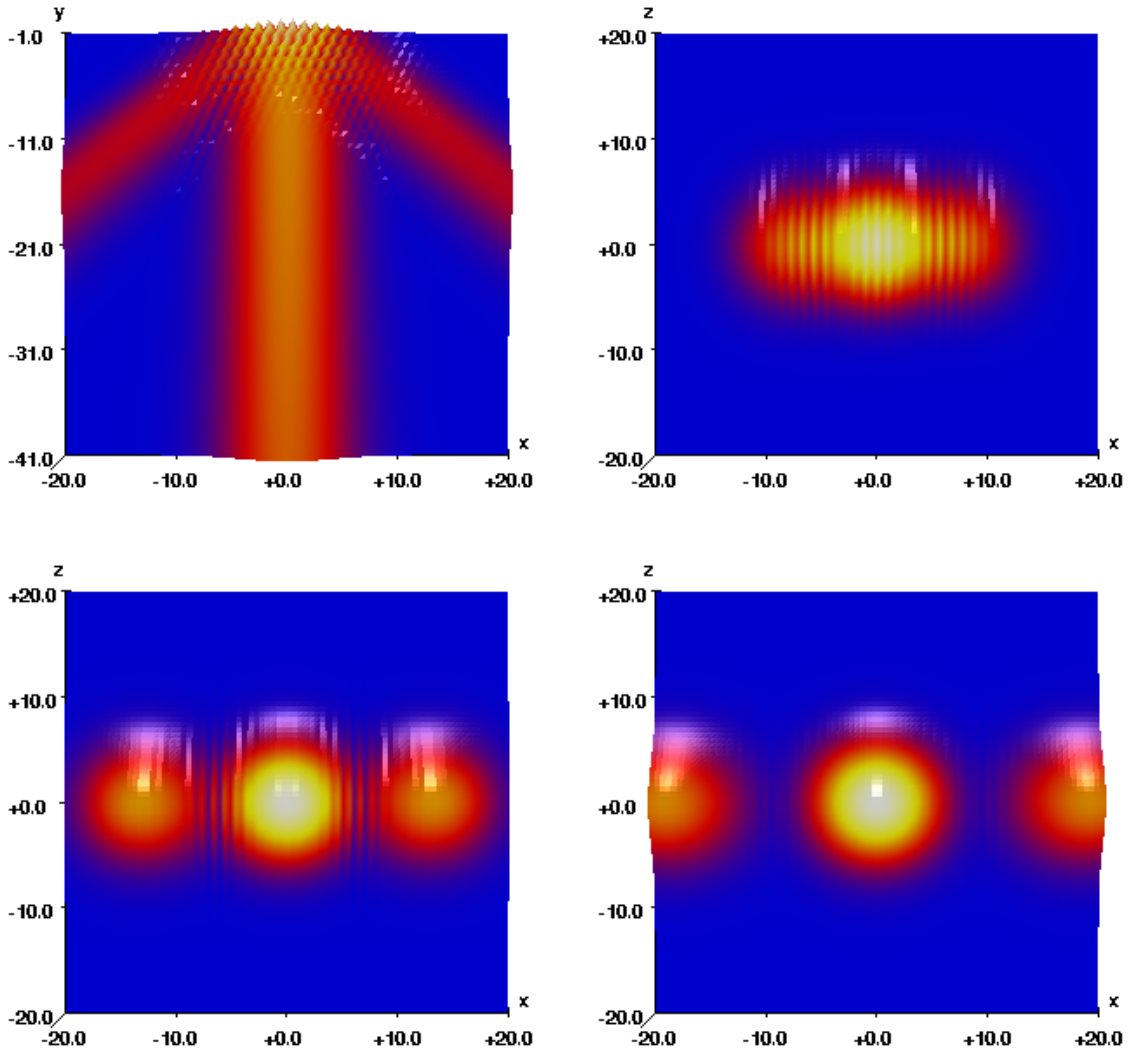


Figure 4: Field intensity of transmitted Gaussian beam in $\{x_3 = 0\}$ plane (upper left) and in planes $\{x_2 = c\}$ with $c = -5d$ (upper right), $c = -10d$ (lower left) and $c = -15d$ (lower right)

The next Figure 5 corresponds to the illumination by a radially polarized Gaussian beam of wave length $\lambda = 880$ nm with normal incidence. The tangential components $\mathbf{E}_1^{inc}, \mathbf{E}_3^{inc}$ in the plane $(x_1, 10d, x_3)$ are

given by

$$(\mathbf{E}_1^{inc}, \mathbf{E}_3^{inc})(x_1, x_3) = -\frac{(x_1, x_3)}{\sqrt{x_1^2 + x_3^2}} e^{-(x_1^2 + x_3^2)/3d}.$$

Then the \mathbf{E} -field of the radially polarized Gaussian beam is given by the integral (2.1) with

$$\mathbf{F}(x_1, x_3) = (\mathbf{E}_3^{inc}(x_1, x_3), 0, -\mathbf{E}_1^{inc}(x_1, x_3))^T = \frac{e^{-(x_1^2 + x_3^2)/3d}}{\sqrt{x_1^2 + x_3^2}} (-x_3, 0, x_1)^T.$$

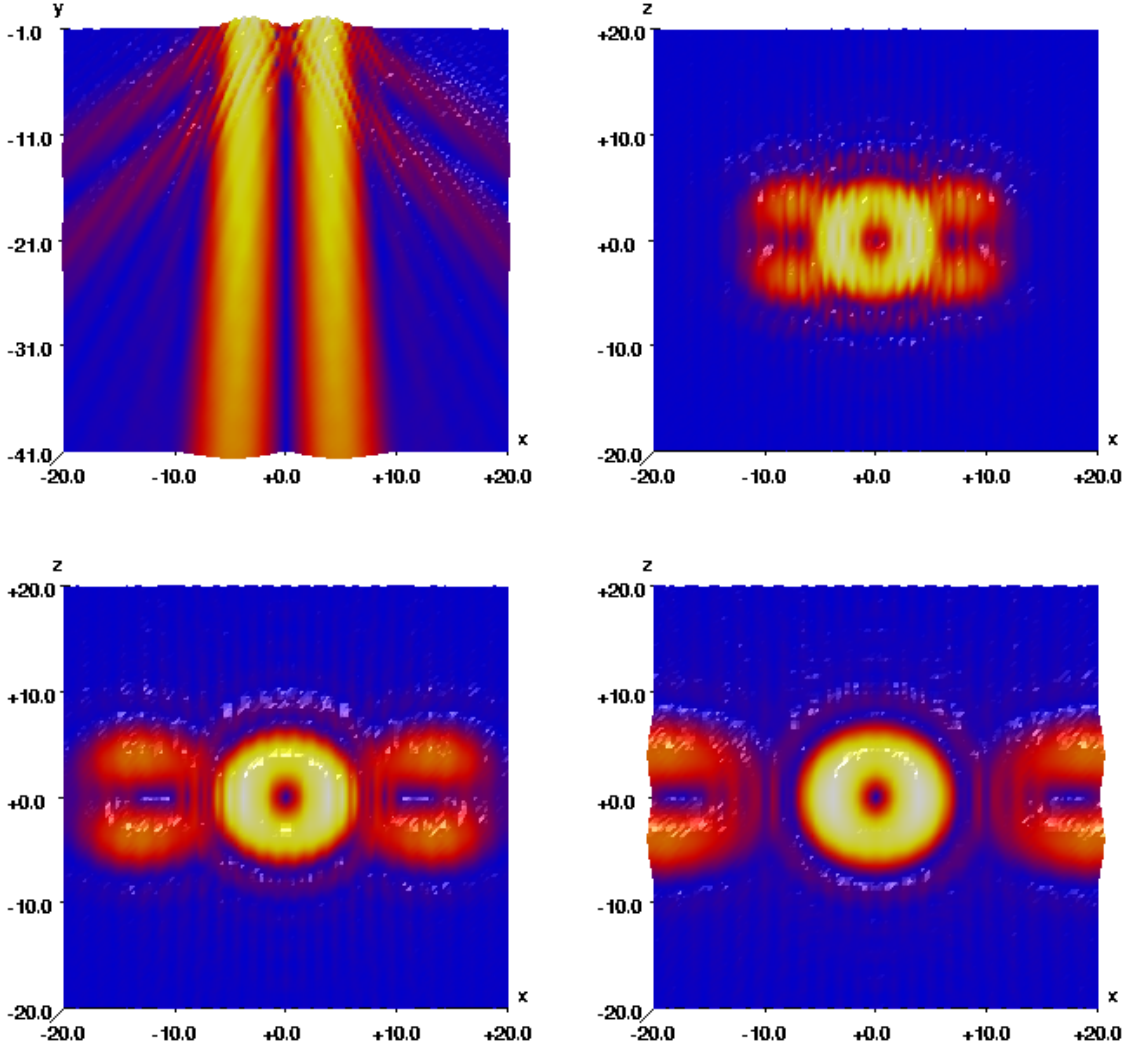


Figure 5: Field intensity below of transmitted radially polarized Gaussian beam in $\{x_3 = 0\}$ plane (upper left) and in planes $\{x_2 = c\}$ $c = -5d$ (upper right), $c = -10d$ (lower left) and $c = -15d$ (lower right)

Figure 6 corresponds to the illumination by a plane wave passing through a circular aperture of radius $5d$ with the wave length $\lambda = 880$ nm and normal incidence. The incident \mathbf{E} -field is given by the integral (2.1) with $H_i = 10d$ and the functions

$$F_1(x_1, x_3) = \Theta_{3d}(x_1, x_3), \quad F_3(x_1, x_3) = i\Theta_{3d}(x_1, x_3),$$

where $\Theta_r(x_1, x_3)$ is the characteristic function of the disc $\{x_1^2 + x_3^2 \leq r^2\}$.

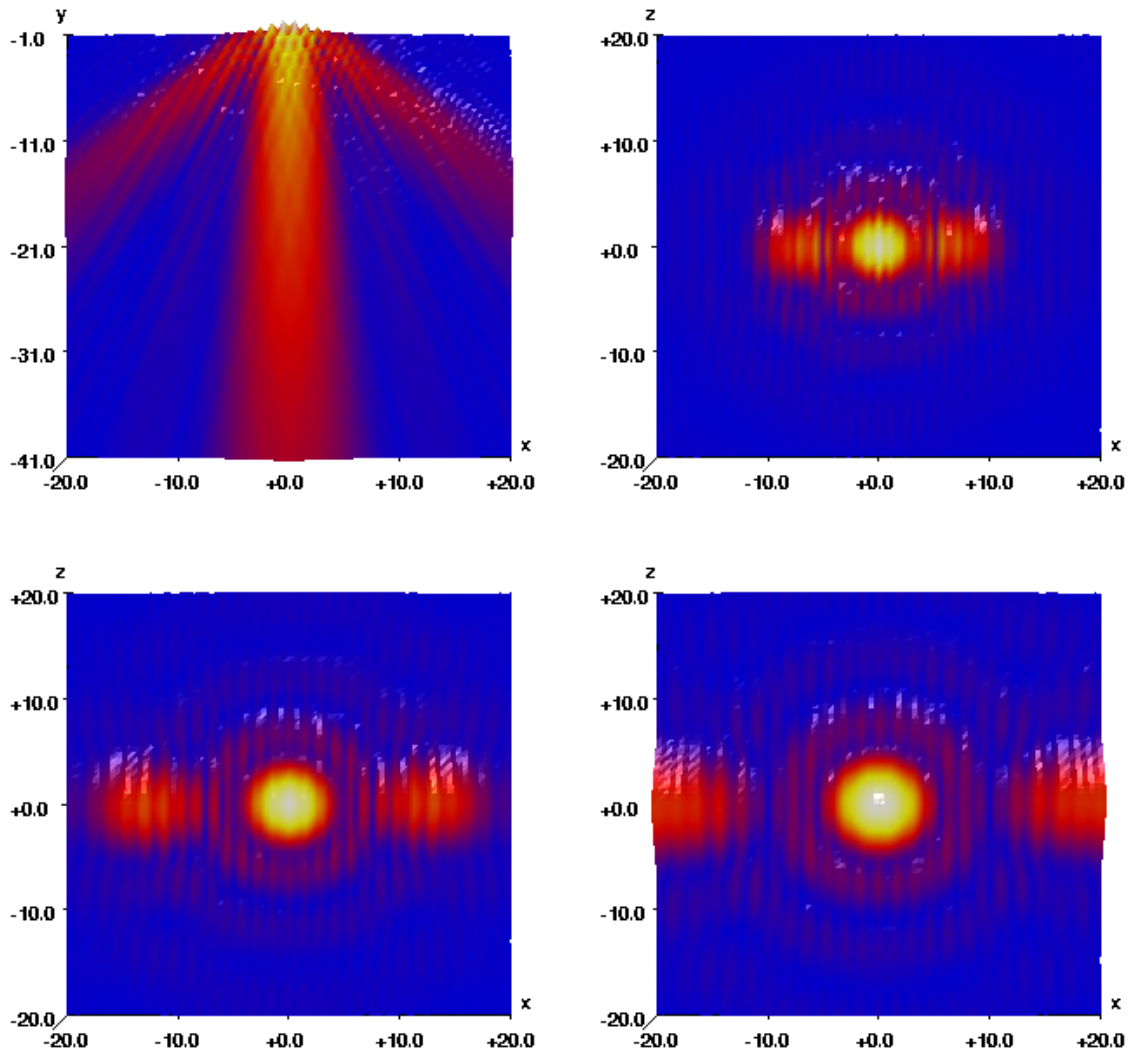


Figure 6: Field intensity of illumination through a circular aperture in $\{x_3 = 0\}$ plane (upper left) and in planes $\{x_2 = c\}$ $c = -5d$ (upper right), $c = -10d$ (lower left) and $c = -15d$ (lower right)

References

- [1] J. Berntsen, T. Espelid, A. Genz, Algorithm 698: DCUHRE: An adaptive multidimensional integration routine for a vector of integrals, ACM Trans. Math. Softw. 17, 452-456 (1991)
- [2] J. Berntsen, T. Espelid, A. Genz, An adaptive algorithm for the approximate calculation of multiple integrals ACM Trans. Math. Softw. 17, 437-45 (1991)
- [3] J. Bischoff, W. Neundorff, Effektive schema for the rigorous modeling of grating diffraction with focused beams, Appl. Optics, Volume 50, Nr. 16, 2474-2483 (2011)
- [4] R. Cools and A. Haegemans. Algorithm 824: CUBPACK: A package for automatic cubature; Framework description. ACM Trans. Math. Softw. 29, 287-296 (2003)

- [5] Elschner, J., Hinder, R., Penzel, F., Schmidt, G., Existence, uniqueness and regularity for solutions of the conical diffraction problem, *Math. Mod. Meth. Appl. Sci.* 10, 317-341 (2000)
- [6] M. Festa, A. Sommariva, Computing almost minimal formulas on the square, *J. Comput. Appl. Math.* 236, 4296-4302 (2012)
- [7] A. Genz, R. Cools, An adaptive numerical cubature algorithm for simplices, *ACM Trans. Math. Softw.* 29, 297-308 (2003)
- [8] L. Goray, G. Schmidt, Solving conical diffraction grating problems with integral equations, *J. Opt. Soc. Am. A* 27, 585-597 (2010).
- [9] L. Goray, G. Schmidt, Boundary integral equation methods for conical diffraction and short waves, Chapter 12 in [11]
- [10] I.P. Omelyan, V.B. Solovyan, Improved cubature formulae of high degrees of exactness for the square, *J. of Comp. Appl. Math.* 188, 190-204 (2006)
- [11] E. Popov (ed), *Gratings: Theory and Numeric Applications Second Revisited Edition*, Institut Fresnel, AMU (2014)
- [12] <http://www.feynarts.de/cuba/>
- [13] G. Schmidt, Conical diffraction by multilayer gratings: a recursive integral equation approach, *Appl. of Math.*, 58, 279-307, (2013)
- [14] G. Schmidt, Boundary Integral Methods for Periodic Scattering Problems. In: A. Laptev (ed.), *Around the Research of Vladimir Maz'ya II. Partial Differential Equations*, IMS 12, Springer: New York, 337-364 (2010)
- [15] G. Schmidt, B. Kleemann, Integral equation methods from grating theory to photonics: An overview and new approaches for conical diffraction, *J. of Mod. Optics* 58, 407-423 (2011)
- [16] K. Watanabe, Two-dimensional electromagnetic scattering of non-plane incident waves by periodic structures, *PIER* 74, 241-271 (2007)
- [17] S. Wu, T. Gaylord, E. Glytsis and Y. Wu, Three-dimensional converging-diverging Gaussian beam diffraction by a volume grating, *J. Opt. Soc. Am. A* Vol. 22, 1293-1303 (2005)
- [18] S. Zhang , F. Wyrowski and J. Tervo, Efficient grating simulation for general incident beam, *Proc. SPIE* 8977, 1-12 (2014).